

# Experimental and Theoretical Evidence of an S<sub>N</sub>2-Type Mechanism for Dissociation of B–N Coordination Bonds in 2,6-Bis((dimethylamino)methyl)phenylborane Derivatives<sup>1</sup>

Shinji Toyota,\* Tadahiro Futawaka, Mitsuhiro Asakura, Hiroshi Ikeda, and Michinori Ōki

Department of Chemistry, Faculty of Science, Okayama University of Science, Ridaicho, Okayama 700-0005, Japan

Received May 18, 1998

To distinguish between dissociation of a B–N coordination bond by S<sub>N</sub>1- and S<sub>N</sub>2-type mechanisms, two series of 1,3,2-dioxaborolanes (boronates) and BEt<sub>2</sub> (borane) complexes carrying a 2,6-bis((dimethylamino)methyl)phenyl group as a third substituent were synthesized by the reaction of the corresponding organolithium compound with an appropriate boron reagent. In the solid state, the boronate complex exhibits a structure in which only one NMe<sub>2</sub> group is coordinated to a tetracoordinated boron atom according to the X-ray analysis and the solid-state NMR. In solution there is a rapid exchange between the coordinated and uncoordinated amine ligands. The barriers to B–N dissociation in the boronate and borane complexes are lower by >3.4 and 6.6 kcal/mol than in the corresponding monoamino complexes, respectively, which is due to electronic assistance in an S<sub>N</sub>2-type mechanism. This observation is supported by ab initio calculations for the system of NH<sub>3</sub> and BH<sub>3</sub>. The dynamic process observed in the boronate complex with 4,4-diphenyl substituents is also discussed.

## Introduction

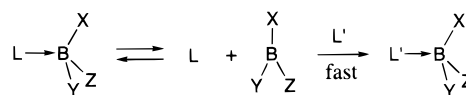
While the reaction mechanisms of nucleophilic substitutions at tetrahedral sp<sup>3</sup> carbon atoms have been comprehensively studied, there have been few systematic studies of those at tetracoordinated boron atoms, which are isoelectronic to carbons in methane-type compounds. It is reasonable to assume that the established classification of the S<sub>N</sub> reactions in the carbon chemistry, unimolecular (S<sub>N</sub>1) and bimolecular (S<sub>N</sub>2) mechanisms, is applicable to the boron chemistry because of the electronic similarity (Scheme 1).

The S<sub>N</sub>1-type mechanism is widely accepted for the exchange reactions of borane–Lewis base complexes in the presence of excess Lewis bases in solutions.<sup>2,3</sup> For instance, in the reaction system of the Me<sub>3</sub>N:BM<sub>2</sub> complex, the exchange between the coordinated and free amine ligands proceeds by the dissociative mechanism, in which the dissociation of the B–N coordination bond is the rate-limiting step.<sup>2</sup>

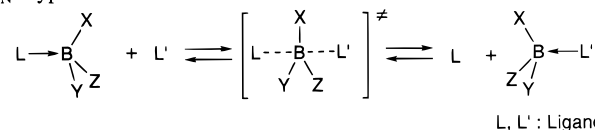
Although there are some examples of the S<sub>N</sub>2-type mechanism in the gas-phase reactions of the BH<sub>3</sub>:CO complex,<sup>4</sup> little is known about the mechanism for the substitution at tetracoordinated boron atoms, especially in solutions. In 1990, Müller and Bürgi proposed an

## Scheme 1

S<sub>N</sub>1-type mechanism



S<sub>N</sub>2-type mechanism



S<sub>N</sub>2 mechanism for the replacement of the intramolecularly coordinated amine ligand by an external pyridine ligands in a tripod-shaped complex, 2,2',2''-nitrotriphénol borate, on the basis of the thermodynamic and kinetic data of the exchange process.<sup>5</sup>

Our previous work has shown that the dissociation of the intramolecular B–N coordination bond in **1b** was a slightly but significantly accelerated in nucleophilic solvents such as ether and acetone with respect to what is expected from their polarity due to a contribution of S<sub>N</sub>2-type mechanism.<sup>6</sup> This explanation was indirectly supported by the experimental finding that the effect of solvent nucleophilicity became negligible in the 9-borabicyclo[3.3.1]nonane complex (**6**), in which solvent molecules are prevented from approaching the boron center by the bulky substituent.<sup>7</sup>

(1) A part of the results in this paper has been published as a communication: Toyota, S.; Futawaka, T.; Ikeda, H.; Ōki, M. *J. Chem. Soc., Chem. Commun.* **1995**, 2499.

(2) Cowly, A. H.; Mills, J. L. *J. Am. Chem. Soc.* **1969**, *91*, 2911.

(3) Glavincevski, B.; Brownstein, S. K. *Can. J. Chem.* **1980**, *59*, 3012.

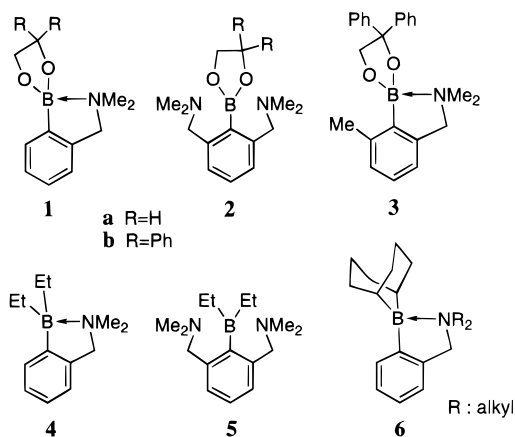
(4) (a) Burg, A. B. *J. Am. Chem. Soc.* **1952**, *74*, 3482. (b) Fu, Y.-C.; Hill, G. R. *J. Am. Chem. Soc.* **1962**, *84*, 353. (c) Grotewold, J.; Lissi, E. A.; Villa, A. E. *J. Chem. Soc. (A)* **1966**, 1034.

(5) Müller, E.; Bürgi, H.-B. *Helv. Chim. Acta* **1987**, *70*, 511.

(6) Toyota, S.; Ōki, M. *Bull. Chem. Soc. Jpn.* **1990**, *63*, 1168.

(7) Toyota, S.; Ōki, M. *Bull. Chem. Soc. Jpn.* **1991**, *64*, 1554.

## Scheme 2

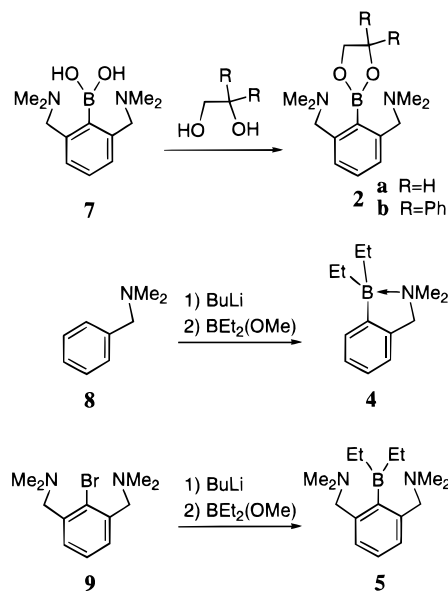


Another approach to verify the mechanism is the introduction of one more amine ligand at the remaining *o*-position in **1**, e.g. using the 2,6-bis((dimethylamino)methyl)phenyl group.<sup>8–12</sup> The second NMe<sub>2</sub> ligand can strongly interact with the boron atom from the rear face of the coordinated boron to amplify the S<sub>N</sub>2-type contribution. Therefore, we synthesized two series of organoboron compounds carrying the terdentate ligand, the boronate (**2**) and borane (**5**) complexes, and the rates of the dissociation of the B–N coordination bonds were determined by spectroscopic methods. The comparison of the kinetic data with those of the corresponding monoamino complexes, **1** and **4**, gave a clear account of the S<sub>N</sub>2-type mechanism for the dissociation.

## Results

The organoboron complexes, **2**, **4**, and **5**, were synthesized according to the reactions in Scheme 3. Compound **3** was prepared in a similar manner as the preparation of **1**.<sup>6,10b,13</sup> In contrast to ligand-free trialkylboranes, which are liable to decomposition, **4** and

## Scheme 3



**5** are stable under ordinary conditions due to the stabilization by the intramolecular coordination.

<sup>11</sup>B NMR showed signals at  $\delta$  15.2 (**1b**)<sup>13</sup> and 14.4 (**2b**) for the boronates and  $\delta$  7.3 (**4**) and 8.0 (**5**) for the borane complexes, referenced to BF<sub>3</sub>·OEt<sub>2</sub> at 0 ppm. The boron atoms in these complexes are more shielded compared with those in the ligand-free reference compounds,  $\delta$  31.2 (2-phenyl-1,3,2-dioxaborolane)<sup>14</sup> and 84.5 (1-phenylborolane),<sup>15</sup> indicating tetracoordinated borons.<sup>16,17</sup> The effect of the second amine ligand on the chemical shift is very small both in the boronate and borane systems.

X-ray analysis of single crystals of **2b** afforded the structure shown in Figure 1, in which one of the two amine ligands coordinates to the boron atom. The <sup>13</sup>C NMR spectrum of **2b** was measured in the solid state by the cross-polarization method: a notable spectral feature is the presence of the two sets of the signals due to the amine ligands, for example the benzylic carbons at  $\delta$  60.9 and 66.0.

**Dynamic Behavior in Solution.** <sup>1</sup>H and <sup>13</sup>C NMR spectra of the organoboron complexes were measured at various temperatures for the observation of the dynamic behavior in solutions.

**(a) Organoboronate Complexes.** In **2a,b**, the two –CH<sub>2</sub>NMe<sub>2</sub> groups were magnetically equivalent even though the temperature was decreased to the lowest attainable temperature, –100 °C, in dichloromethane-*d*<sub>2</sub> or toluene-*d*<sub>8</sub>. The barrier to the site exchange between the two ligands, namely the dissociation of the B–N coordination bond, is estimated to be less than 7.5 kcal/mol.<sup>18</sup>

(14) Odom, J. D.; Moore, T. F.; Goetze, R.; Nöth, H.; Wrackmeyer, B. *J. Organomet. Chem.* **1979**, *173*, 15.

(15) Wrackmeyer, B.; Goetze, R.; Nöth, H. *Chem. Ber.* **1976**, *109*, 1075.

(16) Kidd, R. G. In *NMR of Newly Accessible Nuclei*; Laszlo, P., Ed.; Academic Press: London, 1983; Vol. 2, Chapter 3.

(17) Odom, J. D. In *Comprehensive Organometallic Chemistry*; Wilkinson, G.; Stone, F. G. A., Abel, E. W., Eds.; Pergamon Press: Oxford, U.K., 1992; Chapter 5.1.

(18) The averaged signals means that the rate constant of the exchange between the two ligands is more than 10<sup>3</sup> at –100 °C on the basis of the NMR time scale and the chemical shift difference observed in the solid-state NMR. These values give the upper limit of the free energy of activation.

(8) (a) Grove, D. M.; van Koten, G.; Louwen, J. N.; Noltes, J. G.; Spek, A. L.; Ubbels, H. J. C. *J. Am. Chem. Soc.* **1982**, *104*, 6609. (b) van Koten, G.; Jastrzebski, J. T. B. H.; Noltes, J. G.; Spek, A. L.; Schoone, J. C. *J. Organomet. Chem.* **1978**, *148*, 233. (c) Jastrzebski, J. H. B. H.; van der Schaaf, P. A.; Boersma, J.; van Koten, G.; Zoutberg, M. C.; Heijdenrijk, D. *Organometallics* **1989**, *8*, 1373. (d) van Koten, G. *Pure Appl. Chem.* **1989**, *61*, 1697. (e) Atwood, D. A.; Cowley, A. H.; Ruiz, J. *Inorg. Chim. Acta* **1992**, *198–200*, 271. (f) Chui, C.; Corriu, R. J. P.; Mehdi, A.; Reyé, C. *Angew. Chem., Int. Ed. Engl.* **1993**, *32*, 1311. (g) Benin, V. A.; Martin, J. C.; Willcott, M. R. *Tetrahedron Lett.* **1994**, *35*, 2133. (h) Yamamoto, Y.; Chen, X.; Kojima, S.; Ohdoi, K.; Kitano, M.; Doi, Y.; Akiba, K.-y. *J. Am. Chem. Soc.* **1995**, *117*, 3922. (i) Yoshifujii, M.; Otoguro, A.; Toyota, K. *Bull. Chem. Soc. Jpn.* **1994**, *67*, 1503.

(9) (a) Schumann, H.; Wassermann, W.; Dietrich, A. *J. Organomet. Chem.* **1989**, *365*, 11. (b) Cowley, A. H.; Jones, R. A.; Mardones, M. A.; Ruiz, J.; Atwood, J. L.; Bott, S. G. *Angew. Chem., Int. Ed. Engl.* **1990**, *29*, 1150. (c) Schumann, H.; Hartmann, U.; Wassermann, W. *Chem. Ber.* **1991**, *124*, 1567. (d) Contreras, L.; Cowley, A. H.; Gabbai, F. P.; Jones, R. A.; Carrano, C. J.; Bond, M. R. *J. Organomet. Chem.* **1995**, *489*, C1. (e) Cowley, A. H.; Gabbai, F. P.; Isom, H. S.; Decken, A. *J. Organomet. Chem.* **1995**, *500*, 81.

(10) (a) Lauer, M.; Wulff, G. *J. Organomet. Chem.* **1983**, *256*, 1. (b) Lauer, M.; Böhnke, H.; Grotstollen, R.; Salehnia, M.; Wulff, G. *Chem. Ber.* **1985**, *118*, 246.

(11) Schlenger, R.; Sieler, J.; Jelonek, S.; Hey-Hawkins, E. *J. Chem. Soc., Chem. Commun.* **1997**, 197.

(12) (a) van Beek, J. A. M.; van Koten, G.; Smeets, W. J. J.; Spek, A. L. *J. Am. Chem. Soc.* **1986**, *108*, 5010. (b) van der Kuil, L. A.; Luitjes, H.; Grove, D. M.; Zwikker, J. W.; van der Linden, J. G. M.; Roelofsen, A. M.; Jenneskens, L. W.; Drenth, W.; van Koten, G. *Organometallics* **1994**, *13*, 468. (c) Steenwinkel, P.; James, S. L.; Grove, D. M.; Veldman, N.; Spek, A. L.; van Koten, G. *Chem. Eur.* **1996**, *2*, 1440.

(13) Burgemeister, T.; Grobe-Einsler, R.; Grotstollen, R.; Mannschreck, A.; Wulff, G. *Chem. Ber.* **1981**, *114*, 3403.

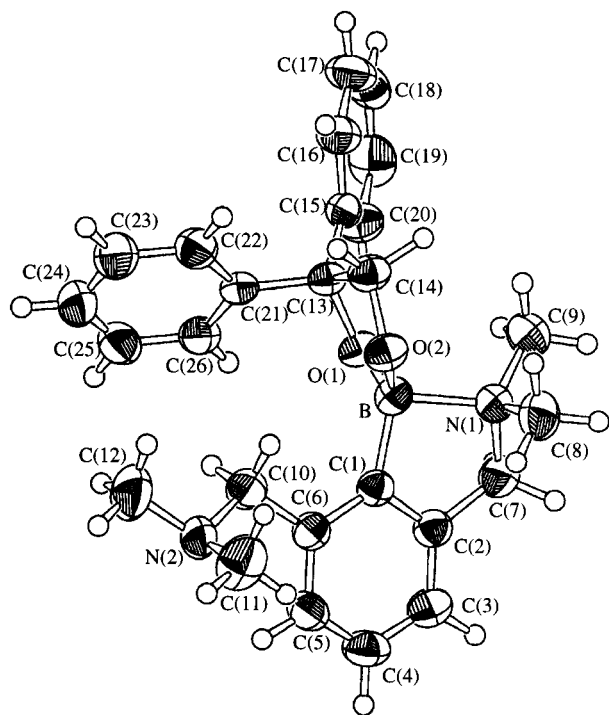


**Figure 1.** ORTEP drawing of **2b** (50% probability ellipsoids). Selected structural parameters: N(1)–B 1.762(3), C(1)–B 1.599(3), O(1)–B 1.443(3), O(2)–B 1.432(2) Å; C(1)–B–O(1) 116.1(2), C(1)–B–O(2) 121.0(2), O(1)–B–O(2) 107.4(2), N(1)–B–C(1) 96.2(1), N(1)–B–O(1) 106.3(1), N(1)–B–O(2) 108.0(2)<sup>°</sup>; tetrahedral character<sup>26</sup> 49%.

**Table 1. Kinetic Parameters for Site Exchange of Diastereotopic Benzylic Methylene Protons in **2b** in Various Solvents**

solvent ( $\epsilon$ ) <sup>a</sup>	$\Delta H^\ddagger$ (kcal/mol)	$\Delta S^\ddagger$ (cal/(mol·K))	$\Delta G^\ddagger_{273}$ (kcal/mol)
C <sub>6</sub> D <sub>11</sub> CD <sub>3</sub> (2.0)	14.4 ± 0.3	7.7 ± 1.1	12.3
C <sub>6</sub> D <sub>5</sub> CD <sub>3</sub> (2.4)	15.3 ± 0.3	8.3 ± 1.1	13.0
CD <sub>2</sub> Cl <sub>2</sub> (8.9)	16.1 ± 0.4	9.8 ± 1.2	13.4
CD <sub>3</sub> COCD <sub>3</sub> (20.6)	17.0 ± 0.2	13.3 ± 0.7	13.4
(CD <sub>3</sub> ) <sub>2</sub> NCDO (36.7)	20.8 ± 0.3	24.2 ± 0.9	14.2

<sup>a</sup> Dielectric constants taken from ref 19.

Compound **2a** showed no line shape changes due to the temperature in any of the <sup>1</sup>H and <sup>13</sup>C NMR spectra. **2a** gave three singlets in the aliphatic region at 2.41, 3.60, and 4.10 ppm for the *N*-methyl (*N*-Me), the benzylic methylene (*N*-CH<sub>2</sub>), and the methylene protons in the 1,3,2-dioxaborolane ring (*O*-CH<sub>2</sub>), respectively.

While compound **2b** gave three singlets in the aliphatic region at 2.16 (*N*-Me), 3.49 (*N*-CH<sub>2</sub>), and 4.81 (*O*-CH<sub>2</sub>) at room temperature, only the signal due to the *N*-CH<sub>2</sub> protons broadened and finally split into an AB quartet at low temperatures. The other proton signals as well as all the carbon signals were unchanged during the temperature change. The line shape change of the *N*-CH<sub>2</sub> signals was analyzed by the total line shape analysis to afford the kinetic data of the site exchange of the diastereotopic protons (Table 1).

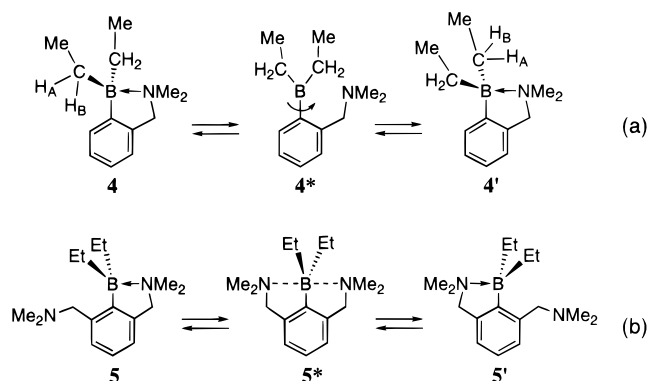
The kinetic parameters for the dissociation of the B–N bond in compound **3**, which has an extra methyl group at the 6-position with respect to **1**, were similarly

**Table 2. Kinetic Parameters for Dissociation of the B–N Coordination Bond in Intramolecular Boronate–Amine and Borane–Amine Complexes**

compd	solvent	$\Delta H^\ddagger$ (kcal/mol)	$\Delta S^\ddagger$ (cal/(mol·K))	$\Delta G^\ddagger_{273}$ (kcal/mol)
<b>1b</b> <sup>a</sup>	CD <sub>2</sub> Cl <sub>2</sub>	15.2 ± 0.3	15.6 ± 1.1	10.9
<b>2b</b>	CD <sub>2</sub> Cl <sub>2</sub>			< 7.5
<b>3</b>	CD <sub>2</sub> Cl <sub>2</sub>	15.2 ± 0.3	10.5 ± 1.1	12.3
<b>4</b>	C <sub>2</sub> D <sub>2</sub> Cl <sub>4</sub>	14.2 ± 0.4	–16.2 ± 1.1	18.6
<b>5</b>	CD <sub>2</sub> Cl <sub>2</sub>	13.8 ± 0.2	6.6 ± 0.9	12.0

<sup>a</sup> Reference 6.

**Scheme 4**



determined by the line shape change of the *N*-CH<sub>2</sub> signals (Table 2).<sup>6</sup>

**(b) Organoborane Complexes.** In complex **4**, the signal due to the methylene protons in the *B*-ethyl groups appeared as an AB part of the ABX<sub>3</sub> system because of the tight B–N coordination. These signals were kept unchanged until the temperature was raised to 70 °C, and the line broadening was observed at higher temperatures. The line shape analysis afforded rates of the dissociation of the B–N bond; the methylene protons exchange their sites with each other after the dissociation of the B–N bond and the facile rotation of the –BEt<sub>2</sub> moiety followed by the recombination of the coordination bond (Scheme 4a).

Complex **5** afforded only one set of proton signals due to the –CH<sub>2</sub>NMe<sub>2</sub> groups at  $\delta$  2.42 (*N*-Me) and 3.71 (*N*-CH<sub>2</sub>) at room temperature. As the temperature was lowered, these signals broadened, decoalesced, and finally separated into two singlets with 1:1 intensity at –60 °C in dichloromethane-*d*<sub>2</sub>, these being assignable to the coordinated and uncoordinated ligands as discussed later. During the temperature change, the aromatic signals also showed the line shape change from an A<sub>2</sub>B to an ABC pattern. The rates of the exchange of the two ligands (Scheme 4b) were obtained by the analysis of the *N*-Me and *N*-CH<sub>2</sub> signals, which gave the same results within experimental errors (Table 2).

**Ab Initio Calculation.** To provide support to the mechanisms of the dissociation of the B–N coordination bonds, we carried out ab initio calculations for simplified model reactions comprised of borane (BH<sub>3</sub>) and ammonia (NH<sub>3</sub>) molecules as shown in Scheme 5.

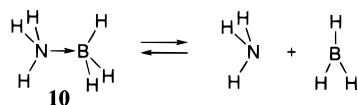
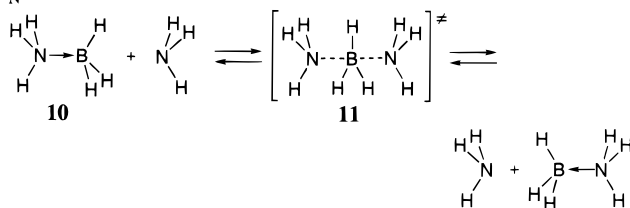
In the S<sub>N</sub>1 mechanism, the initial state is a 1:1 borane–ammonia complex (**10**) and the transition state is modeled by the dissociated species, an ammonia and a borane molecule. The energy difference between the initial and transition states can be regarded as the barrier to the S<sub>N</sub>1-type dissociation, being identical with



**Table 3.** Calculated Activation Energy for  $S_N1$ - and  $S_N2$ -Type Model Reactions, B–N Interatomic Distances, and Atomic Charges in 1:1 and 1:2 Borane–Ammonia Complexes<sup>a</sup>

borane	method <sup>b</sup>	$E_a(S_N1)$	$E_a(S_N2)$	$\Delta E_a^c$	$H_3N-BR_3$		$H_3N-BR_3-NH_3$	
					$r_{B-N}^d$	$q^e$	$r_{B-N}^d$	$q^e$
BH <sub>3</sub>	HF//HF	23.5	11.6	11.9	1.689	-0.262	2.427	-0.085
BH <sub>3</sub>	MP2//HF	34.3	15.1	19.2	1.689	-0.262	2.427	-0.085
BH <sub>3</sub>	MP2//MP2	34.4	13.6	20.8	1.664	-0.273	2.215	-0.116
BH <sub>3</sub>	MP3//MP3	33.1	13.8	19.3	1.665	-0.268	2.245	-0.110
BH <sub>2</sub> Me	MP2//HF	29.4	16.7	12.7	1.700	-0.238	2.624	-0.048
BHMe <sub>2</sub>	MP2//HF	25.4	17.2	8.2	1.718	-0.209	2.954	-0.026
BMe <sub>3</sub>	MP2//HF	22.5	16.7	5.8	1.738	-0.179	3.353	-0.021

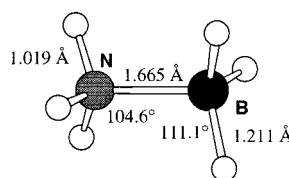
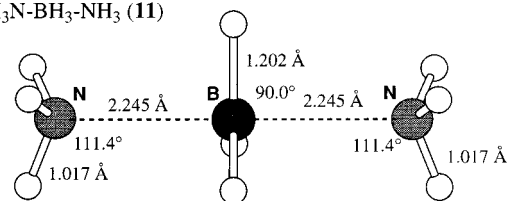
<sup>a</sup> Energies ( $E$ ) in kcal/mol. <sup>b</sup> Basis set at 6-31G\*. <sup>c</sup>  $\Delta E_a = E_a(S_N1) - E_a(S_N2)$ . <sup>d</sup> Interatomic distances between B and N atoms in Å. <sup>e</sup> Sum of atomic charges on the BR<sub>3</sub> group. The atomic charges on the NH<sub>3</sub> group are  $-q$  and  $-0.5q$  for the 1:1 and 1:2 complexes, respectively.

**Scheme 5** $S_N1$  model $S_N2$  model

the dissociation energy of the B–N coordination bond.<sup>20</sup> For the  $S_N2$  mechanism, a trigonal bipyramidal (TBP) transition state with two NH<sub>3</sub> molecules at the apical positions (**11**) is assumed. The activation energy of the  $S_N2$ -type reaction is calculated by subtracting the total energy of a 1:1 complex and that of an ammonia molecule from that of the 1:2 complex.

The calculations were carried out with the 6-31G\* basis set at the HF or MP level. The results are listed in Table 3. The optimized structures of 1:1 and 1:2 complexes calculated at the highest level (MP3/6-31G\*) are shown in Figure 2, with selected structural parameters and total energies.

There have been several reports on the theoretical calculation of the 1:1 complex (**10**), and our results are consistent with them.<sup>21–23</sup> The molecule has  $C_{3v}$  symmetry, and the BH<sub>3</sub> moiety carries the negative charge of  $-0.27e$  to form a coordination bond with partial ionic character. As pointed in the literature,<sup>21,22</sup> the struc-

 $H_3N-BH_3$  (**10**)– 82.89771 Hartree ( $C_{3v}$ ) $H_3N-BH_3-NH_3$  (**11**)– 139.24166 Hartree ( $D_{3h}$ )**Figure 2.** Optimized structures and total energies of borane–ammonia complexes **10** and **11** calculated at MP3/6-31G\*. (The total energies of BH<sub>3</sub> and NH<sub>3</sub> are  $-26.47907$  and  $-56.36595$  Hartree, respectively, at the same level.)

ture and energy are in good agreement with the experimental values,  $r_{B-N}$  1.657 Å (gas phase)<sup>24</sup> and  $E_a = 31.1$  kcal/mol,<sup>25</sup> when the electron correlation is applied.

The 1:2 complex (**11**) was optimized in  $D_{3h}$  symmetry as the transition state which is indicated by one imaginary value in wavenumbers. The distance between the central boron atom and the nitrogen at the apical position is 2.245 Å, and the calculated activation energy is 19.3 kcal/mol at the MP3/6-31G\* level. Although the effect of the electron correlation on the geometry of the 1:2 complex is large, that on the energy level is rather small.

Because the model reaction mentioned above may be oversimplified, the intramolecular model of **12**, of which structure is similar to **2** and **5**, was also calculated. We abandoned the electron correlation due to computational limitation, and these structures and energies were obtained at the HF/3-21G\* level. The tetracoordinated form (**12a**) (Scheme 6) gave the lowest energy among the various coordination bonds. The pentacoordinated structure (**12b**) is regarded as the transition state of the  $S_N2$ -type mechanism, being less stable by 7.9 kcal/mol

(20) Strictly, the dissociated species, borane and ammonia, are not in the transition state in the model of the  $S_N1$ -type mechanism, where the total energy constantly increases as the two molecules move away from each other. We expect that the transition state lies at the late stage in the dissociation process in the actual cases because the dissociation is an endothermic process. Therefore, the energies calculated for the model reaction are not so far from the real activation energies.

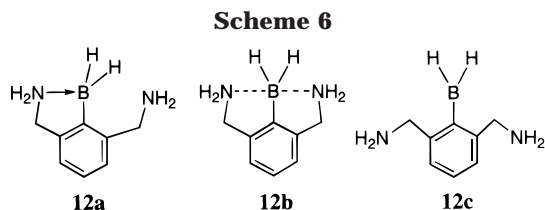
(21) Jonas, V.; Frenking, G.; Reetz, M. T. *J. Am. Chem. Soc.* **1994**, *116*, 8741. Jonas, V.; Frenking, G. *J. Chem. Soc., Chem. Commun.* **1994**, 1489.

(22) Hehre, W. J.; Radom, L.; Schleyer, P. v. R.; Pople, J. A. *Ab Initio Molecular Orbital Theory*; John Wiley & Sons: New York, 1986; pp 212–223.

(23) Schleyer et al. pointed out that the B–N distance in the  $H_3B-NH_3$  complex is sensitive against the calculation method and experimental conditions because its potential surface is quite flat: Bühl, M.; Steinke, T.; Schleyer, P. v. R.; Boese, R. *Angew. Chem., Int. Ed. Engl.* **1991**, *30*, 1160.

(24) Thorne, L. R.; Suenram, R. D.; Lovas, F. J. *J. Chem. Phys.* **1983**, *78*, 167.

(25) Haaland, A. *Angew. Chem., Int. Ed. Engl.* **1989**, *28*, 992.



than **12a**. The structure without intramolecular coordination (**12c**) is at the energy level higher by 29.4 kcal/mol than **12a**, this value being equivalent to the dissociation energy of the B–N bond via the S<sub>N</sub>1-type mechanism.

### Discussion

**Structure of Boronate Complexes in the Solid State.** The X-ray structure of **2b** shows that the boron atom takes a tetraordinated geometry with one coordinated amine ligand and another uncoordinated, which is away from the boron center. This structure is consistent with the solid-state <sup>13</sup>C NMR spectrum, where the signals due to the coordinated and uncoordinated ligands are observed separately. In the solid state, the structure of the molecules are virtually frozen in the tetraordinated form.

The B–N bond length in **2b** of 1.762 Å is comparable to that of the monoamino complex (**1b**) (1.754 Å).<sup>26</sup> The B–N bond length is not always correlated with the strength of the coordination bond in this type of complexes. To correlate the molecular geometry with the strength of coordination bonds in borane–Lewis base complexes, we proposed a structural parameter called “tetrahedral character”, which is an indication of geometrical change from trigonal to tetrahedral structures calculated from the bond angles at boron atoms.<sup>26</sup> The value for **2b** (49%) is comparable to that for **1b** (51%),<sup>26</sup> this indicating that the energies of the B–N coordination bonds are almost the same in the two compounds.

**Experimental Evidence of the S<sub>N</sub>2-Type Mechanism.** The similarity of the <sup>11</sup>B NMR chemical shifts strongly indicates that the boron atoms are tetraordinated in **2** and **5** in solution as they are in **1** and **4**. If the boron atom were to take a pentacoordinated structure, in which the two ligands concurrently interact with the boron atom, the <sup>11</sup>B NMR signal should have shifted downfield compared with those of the tetraordinated compounds.<sup>27</sup>

Therefore, the magnetic equivalence of the two –CH<sub>2</sub>–NMe<sub>2</sub> groups in **2** is attributable to the facile exchange between the coordinated and uncoordinated ones. The estimated upper limit of the barrier to the dissociation in **2b** is lower by 3.4 kcal/mol than the barrier in **1b**. In the borane system, where the coordination is tight due to the strong Lewis acidity, the second amine ligand lowers the barrier by 6.6 kcal/mol at 273 K; in other words, the B–N bond in **5** dissociates faster by the order of 10<sup>5</sup> than that in **4**.

Among various factors in the substituent effect of the second –CH<sub>2</sub>–NMe<sub>2</sub> group on the rates of dissociation, neither the steric nor inductive effect can be significant.

To verify this point, compound **3** was taken as a reference compound; the substituent parameters of the methyl group are similar to those of aminomethyl group,<sup>28</sup> and the steric size of a methyl should be comparable to a –CH<sub>2</sub>NMe<sub>2</sub> group when the amine nitrogen is far away from the boron atom as observed in the X-ray structure. The kinetic data for **1b** and **3** in Table 2 show that the methyl substituent increases the barrier to some extent, being far from decreasing it. The remarkable substituent effect brought by the extra –CH<sub>2</sub>–NMe<sub>2</sub> group must be attributed to other factors.

The structural analysis by means of the tetrahedral character shows that the B–N bond energy in **2** should be comparable to that in the monoamino compound (**1**) as far as the initial state is taken into consideration. Therefore, the facile ligand exchange in **2** is attributable to the substantial lowering of energy of the transition state by the electronic interaction of the extra ligand. We explain this result by an S<sub>N</sub>2-type mechanism, where the uncoordinated ligand assists the dissociation by the approach to the boron atom from the backside of the coordinated ligand (Scheme 7). The TBP structure will be the transition state, and its energy level is much lower than that in the S<sub>N</sub>1 mechanism as discussed with the use of the MO calculation later. As a result, the energy gap between the initial and transition states for the B–N bond dissociation is markedly decreased by the second ligand.

Martin et al. reported a similar phenomenon in the reactions at carbenium ion centers. The exchange between the two possible C–S bonds in the anthracene derivative (**13**) (Scheme 8) occurs much faster than that in the monophenylthio compound,<sup>29a</sup> the S<sub>N</sub>2-type mechanism operating in the former. In a related compound (**14**), the Walden inversion takes place so fast that the central carbon atom behaves as if a pentacoordinated carbon spectroscopically, namely the S<sub>N</sub>2 transition state.<sup>29b</sup> The processes we observed in compounds **2** and **5** are analogous to these reactions at carbon centers and afford clear evidence of the S<sub>N</sub>2 type mechanism in the boron chemistry.

Because the pentacoordinated state of the second-row elements is unstable, it is likely that the structure of **2\*** or **5\*** is the transition state during the substitution process. In fact, there have been no reports on the experimental evidence of hypervalent boron species as stable entities except a special example.<sup>30</sup> Descending the periodic table, we can find several examples of the pentacoordinated structures of Al,<sup>9d</sup> In,<sup>9a,c</sup> and Ga<sup>9b</sup> complexes, where the central atom takes a TBP structure.

**Nature of Dynamic Behavior of **2**.** It is worthwhile mentioning the dynamic behavior of the boronate complexes **2** in more details because the line shape change observed in **2b** is not understood straightforwardly on the basis of the facile exchange of the amine ligands described in the last section. To explain the equivalence of the *O*-CH<sub>2</sub> protons and *N*-Me groups

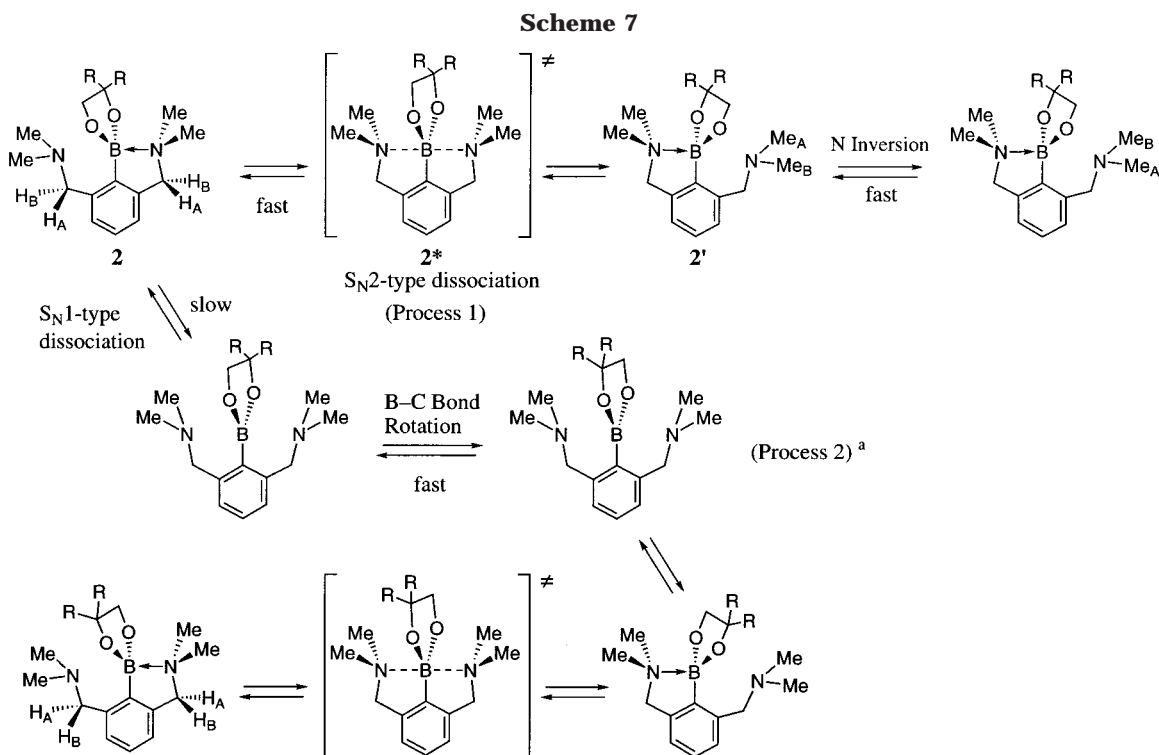
(28) Issacs, N. S. *Physical Organic Chemistry*; Longman Scientific & Technical: Essex, U.K., 1987; Chapter 4.3.

(29) (a) Martin, J. C.; Basalay, R. J. *J. Am. Chem. Soc.* **1973**, *95*, 2572. (b) Forbus, T. R., Jr.; Martin, J. C. *J. Am. Chem. Soc.* **1979**, *101*, 5057.

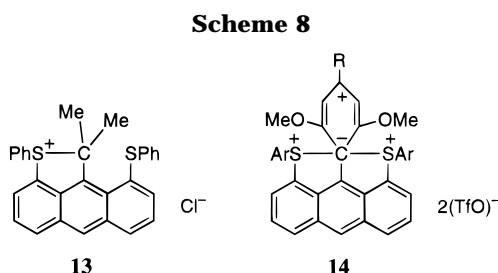
(30) Lee, D. Y.; Martin, J. C. *J. Am. Chem. Soc.* **1984**, *106*, 5745.

(26) Toyota, S.; Ōki, M. *Bull. Chem. Soc. Jpn.* **1992**, *65*, 2857.

(27) The GIAO calculations predict the chemical shift of <sup>11</sup>B NMR as follows: 78.6, –14.5, and 5.5 ppm for BH<sub>3</sub>, **10**, and **11**, respectively.



<sup>a</sup> Only one pathway is shown for Process 2 among several possibilities.



during the site exchange of the *N*-CH<sub>2</sub> protons, other dynamic processes should be taken into consideration. Scheme 7 illustrates the possible processes concerning the site exchange of NMR signals in **2**: the inversion at the free nitrogen atom and the rotation around the B–C<sub>Ph</sub> bond in addition to the dissociation of the B–N coordination bonds.

In the coordinated form of **2b**, the 1,3,2-dioxaborolane (DOB) ring is nearly orthogonal to the attached phenyl moiety, and this conformation makes the magnetic environment of the *N*-CH<sub>2</sub> protons different, one being near the phenyl substituents (H<sub>B</sub>) and the other far away from them (H<sub>A</sub>). The site exchange between H<sub>A</sub> and H<sub>B</sub> is completed after the rotation of the DOB ring by 180°. We postulate that there are two independent processes involved (processes 1 and 2 in Scheme 7).

Because of the facile switching of the two amine ligands, the *O*-CH<sub>2</sub> protons are equivalent and so are the two –CH<sub>2</sub>NMe<sub>2</sub> groups regardless of the direction of the DOB ring (process 1). The site exchange of the two *N*-Me groups at an amine ligand (Me<sub>A</sub> and Me<sub>B</sub>) is achieved by the nitrogen inversion in the uncoordinated ligand, which is usually a fast process for acyclic amines.<sup>31</sup> Furthermore, the fast ligand exchange averages the *N*-Me signals attached to the two amine ligands, so that all the methyl signals appear as a

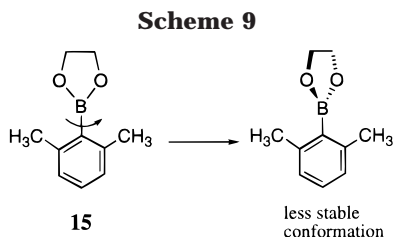
singlet even at low temperatures. Hence, the line shape change of the *N*-CH<sub>2</sub> protons in **2b** must be explained by the slow rotation around the B–C bond.

However, the B–C bond rotation cannot take place directly from the coordinated forms (**2** or **2\***), in which at least one amine ligand interacts with the boron atom to prevent the rotation. It is necessary that both of the two amine ligands dissociate from the boron atom before the DOB ring begins to rotate. Therefore, the dynamic process observed in **2b** is a total of the two steps, the release of the boron atom from the coordination via the dissociation of *S<sub>N</sub>1*-type mechanism and the subsequent B–C bond rotation (process 2).

The next question arises: “Which is the rate-limiting step for process 2?” As discussed in the previous section, the barrier to the dissociation of the B–N bond in **3** is regarded as that of the *S<sub>N</sub>1*-type dissociation in **2b**: the barrier of 12.3 kcal/mol in **3** is comparable to that of the site exchange of the *N*-CH<sub>2</sub> protons in **2b** (13.4 kcal/mol). The rotational barrier around the B–C bond was estimated by ab initio calculation with using a ligand-free model, 2-(2,6-dimethylphenyl)-1,3,2-dioxaborolane (**15**) (Scheme 9), because of the limitation of the experimental approach. At the HF/3-21G\* level, the rotational barrier is only 2.3 kcal/mol and the energy maximum appears at a nearly orthogonal conformation between the phenyl and DOB rings. These results suggest that the rate-limiting step is the dissociation of the B–N bond by the *S<sub>N</sub>1* mechanism rather than the B–C bond rotation.

(31) The barrier to nitrogen inversion is less than 7 kcal/mol for acyclic amines. For example, see: Ōki, M. *Applications of Dynamic NMR Spectroscopy to Organic Chemistry*; VCH Publishers: Deerfield Beach, FL, 1985; Chapter 8. Bushweller, C. H. *Acyclic Organonitrogen Stereodynamics*; Lambert, J., Takeuchi, Y., Eds.; VCH Publishers: New York, 1992; Chapter 1.





This conclusion is also supported by the kinetic data of **2b** in Table 1. Features in the kinetic parameters are the large and positive entropy of activation and the slight acceleration of the dissociation in less polar solvents. From our experience, these are typical for the dissociation of coordination bonds in organoboron complexes;<sup>6,7</sup> the polar coordinated form at the original state is effectively stabilized by solvation relative to the transition state. This kinetic similarity is another piece of evidence that the bond dissociation plays an important role in the dynamic process in **2b**. This mechanism is also consistent with the experimental finding that **2a** showed no line shape changes in the NMR signals. In this compound, the *N*-CH<sub>2</sub> protons are no longer diastereotopic even if the rotation around the B–C bond becomes slow.

We consider that the borane complex (**5**) undergoes a dynamic process similar to the boronate complexes. A different point is that the two amine ligands switch slowly enough to be observable separately at low temperatures because of the strong Lewis acidity of the boron atom in **5**. Although we were not able to obtain kinetic information on the B–C rotation via the S<sub>N</sub>1-type dissociation in **5** due to the lack of appropriate probes, its barrier should be as high as that of the dissociation of the B–N bond in **4**.

**Further Insights into the S<sub>N</sub>2-Type Mechanism by MO Calculation.** In the S<sub>N</sub>2-type mechanism of the model reaction of the borane–ammonia system, the total energy increases constantly as a free ammonia molecule approaches the boron atom from the backside of the coordinated ammonia along the reaction coordinate. The energy has a maximum at the TBP structure (**11**), where two ammonia molecules equally coordinate to the central boron atom. This energy profile of single-maximum is in a marked contrast to that of S<sub>N</sub>2 processes toward carbon centers, where a W-shape energy profile is usually obtained by calculation.<sup>32</sup>

The activation energy of the S<sub>N</sub>2-type reaction is much smaller than that of the S<sub>N</sub>1-type reaction in the borane–ammonia system, the difference being ca. 19 kcal/mol when the electron correlation is applied. The intramolecular model (**12**) also indicates the preference of the S<sub>N</sub>2-type pathway over the S<sub>N</sub>1 by ca. 20 kcal/mol. These mean that the substitution takes place exclusively via the S<sub>N</sub>2 mechanism if the reaction is carried out under ideal conditions such as in gas phase. To extend this conclusion to the experimental cases, we have to consider other kinetic factors, i.e., entropy factor and solvation, as well.

In the borane–ammonia system, the substrate gains additional entropy at the transition state in the S<sub>N</sub>1-

type reaction, where one species separates into two. By contrast, the S<sub>N</sub>2 type mechanism, where two species come together at the transition state, suffers from loss of entropy during the reaction. The vibration analysis estimated the entropy of activation of the S<sub>N</sub>1 and S<sub>N</sub>2 model reactions at 33.5 and –22.1 cal/(mol·K), respectively, at the RHF level. When these values are applied to the reactions at room temperature, the entropy term (*TΔS*<sup>‡</sup>) lowers the free energy of activation for the S<sub>N</sub>1 reaction by ca. 16 kcal/mol relative to that of the S<sub>N</sub>2 reaction. This energy is large enough to compensate the disadvantage of the S<sub>N</sub>1 mechanism in the ammonia–borane system. The entropy factor becomes less significant for the intramolecular reactions such as the compounds we examined in this paper. Therefore, the difference in the calculated activation energies between the S<sub>N</sub>1- and S<sub>N</sub>2-type reactions in the intramolecular model **12** is substantial.

The contribution of the solvation can be discussed by taking advantage of the general concept that the more polar the molecule, the better solvated or stabilized, in a qualitative manner. Among all the species involved in the model reactions of the borane–ammonia system, only the 1:1 complex (**10**) has a large value of the dipole moment (5.62 D, calcd).<sup>33</sup> Because this species is involved in the original state in both the S<sub>N</sub>1- and S<sub>N</sub>2-type mechanisms, the original state is better stabilized by solvation than the transition state to enhance the barrier height, especially in polar solvents. It is difficult to predict in which of the two mechanisms the stabilization works better than the other from the available data.

The calculations for the methyl-substituted boranes afford more information about the substituent effect. The activation energy of the S<sub>N</sub>1 reaction decreases by 3–5 kcal/mol as a hydrogen is substituted by a methyl (Table 3). This tendency is understood by the electron-donating character and the steric effect (F-strain)<sup>34</sup> of the methyl group(s), both of which weaken the Lewis acidity of the boron atom. In contrast, the activation energy of the S<sub>N</sub>2 type mechanism is hardly influenced by the methyl substitution even though the B–N interatomic distance is lengthened by the substitution. On the whole, the activation energy gap between the two mechanisms (*ΔE<sub>a</sub>*) is decreased rapidly in the order of BH<sub>3</sub> > BH<sub>2</sub>Me > BHMe<sub>2</sub> > BMe<sub>3</sub>. This trend is the same as the ease of S<sub>N</sub>2 reaction in the carbon chemistry in the order of methyl > primary > secondary > tertiary carbons. It is worthwhile to mention that the barrier to the S<sub>N</sub>2 reaction is still lower than that to the S<sub>N</sub>1 for the trimethylborane complex.

These theoretical results show that the S<sub>N</sub>2-type mechanism is not the special pathway for the substitution at boron atoms if certain conditions are met. Further calculations will provide more details about the nature of the mechanism including the solvent effect.

## Experimental Section

**General Comments.** <sup>1</sup>H and <sup>13</sup>C NMR spectra were measured on a JEOL GSX-400 or a Bruker ARX-400 spec-

(32) For example: Shaik, S. S.; Schlegel, H. B.; Wolfe, S. *Theoretical Aspects of Physical Organic Chemistry: The S<sub>N</sub>2 Mechanism*; John Wiley & Sons: New York, 1992.

(33) The dipole moments calculated at the MP3/6-31G\* level are 1.97 (1.48) and 5.62 (5.22)<sup>27</sup> D for ammonia and **10**, respectively, with experimental ones in parentheses. The dipole moment is zero for borane and **11**.

(34) Brown, H. C. *J. Am. Chem. Soc.* **1945**, *67*, 378, 1452.

trometer operating at 400 and 100 MHz, respectively.  $^{11}\text{B}$  NMR spectra were measured on the JEOL spectrometer at 128.3 MHz, and the chemical shift was referred to the signal due to  $\text{BF}_3\cdot\text{OEt}_2$  at 0 ppm as an external reference. High-resolution mass spectra were measured on a JEOL JMS-DX303 spectrometer. Melting points were determined with a Mel-Temp apparatus in a capillary and are uncorrected.

**[2,6-Bis((dimethylamino)methyl)phenyl]boronic Acid (7).** This compound was synthesized by the treatment of 1-bromo-2,6-bis((dimethylamino)methyl)benzene<sup>12b</sup> with butyllithium followed by trimethyl borate by the known method:<sup>10a</sup> mp 119–122 °C;  $^1\text{H}$  NMR ( $\text{CDCl}_3$ )  $\delta$  2.34 (s, 12H, *N*-Me), 3.66 (s, 4H, *N*-CH<sub>2</sub>), 5.35 (br, 2H, -OH), 7.01 (d,  $J$  = 7.5 Hz, 2H, 3,5-H), 7.12 (t,  $J$  = 7.4 Hz, 1H, 4-H). Anal. Calcd for  $\text{C}_{12}\text{H}_{21}\text{N}_2\text{BO}_2$ : C, 61.04; H, 8.96; N, 11.86. Found: C, 61.11; H, 9.21; N, 11.79.

**2-[2,6-Bis((dimethylamino)methyl)phenyl]-1,3,2-dioxaborolane (2a).** A solution of 300 mg (1.45 mmol) of the boronic acid (7) and 90 mg (1.45 mmol) of 1,2-ethanediol in 40 mL of toluene was heated under reflux for 2 h. The resulted water was removed azeotropically with a Dean–Stark apparatus. The solvent was removed by evaporation and the residue was recrystallized from hexane to give 298 mg (79%) of the desired compound as colorless crystals: mp 88–89 °C;  $^1\text{H}$  NMR ( $\text{CDCl}_3$ )  $\delta$  2.41 (s, 12H, *N*-Me), 3.69 (s, 4H, *N*-CH<sub>2</sub>), 4.10 (s, 4H, *O*-CH<sub>2</sub>), 7.11 (d,  $J$  = 7.4 Hz, 2H, 3,5-H), 7.20 (t,  $J$  = 7.4 Hz, 1H, 4-H);  $^{13}\text{C}$  NMR ( $\text{CDCl}_3$ )  $\delta$  45.4 (*N*-Me), 63.1 (*N*-CH<sub>2</sub>), 64.7 (*O*-CH<sub>2</sub>), 124.6, 127.9, 141.6 (aromatic carbons);  $^{11}\text{B}$  NMR ( $\text{CDCl}_3$ )  $\delta$  13.9 (line width  $h_{1/2}$  142 Hz). Anal. Calcd for  $\text{C}_{14}\text{H}_{23}\text{N}_2\text{BO}_2$ : C, 64.14; H, 8.84; N, 10.69. Found: C, 63.97; H, 8.95; N, 10.43.

**2-[2,6-Bis((dimethylamino)methyl)phenyl]-4,4-diphenyl-1,3,2-dioxaborolane (2b).** This compound was similarly prepared from 7 and 1,1-diphenyl-1,2-ethanediol<sup>35</sup> in 97% yield: mp 139.5–141.5 °C;  $^1\text{H}$  NMR ( $\text{CDCl}_3$ , rt)  $\delta$  2.16 (s, 12H, *N*-Me), 3.49 (s, 4H, *N*-CH<sub>2</sub>), 4.81 (s, 2H, *O*-CH<sub>2</sub>), 7.12 (d,  $J$  = 7.1 Hz, 2H), 7.14 (2H,  $J$  = 7.3 Hz, t), 7.22 (t,  $J$  = 7.1 Hz, 1H), 7.26 (t,  $J$  = 7.4 Hz, 4H), 7.56 (d,  $J$  = 7.1 Hz, 4H);  $^{13}\text{C}$  NMR ( $\text{CDCl}_3$ )  $\delta$  45.5 (*N*-Me), 63.1 (*N*-CH<sub>2</sub>), 74.5 (*O*-CH<sub>2</sub>), 84.5 (CPh<sub>2</sub>), 124.2, 125.5, 126.2, 127.9, 128.1, 141.8, 148.9 (aromatic carbons);  $^{11}\text{B}$  NMR ( $\text{CDCl}_3$ )  $\delta$  14.4 (line width  $h_{1/2}$  292 Hz). Anal. Calcd for  $\text{C}_{26}\text{H}_{31}\text{N}_2\text{BO}_2$ : C, 75.37; H, 7.54; N, 6.76. Found: C, 75.48; H, 7.65; N, 6.90.

**2-[2-((Dimethylamino)methyl)-6-methylphenyl]-4,4-diphenyl-1,3,2-dioxaborolane (3).** To a solution of 2.94 g (12.9 mmol) of 2-bromo-1-((dimethylamino)methyl)-3-methylbenzene, prepared from 2-bromo-1-(bromomethyl)-3-methylbenzene and dimethylamine, in 30 mL of dry ether was slowly added 8.3 mL (12.9 mmol) of 15% butyllithium in hexane under an argon atmosphere. This solution was stirred for 1 h at room temperature and then was added to a solution of 3.0 mL (26 mmol) of trimethyl borate in 5 mL of ether at -78 °C. The mixture was allowed to warm to room temperature and stirred overnight. After the reflux for 1 h, the volatile materials were evaporated. The residue was extracted with dichloromethane, and the oily extract was purified by the bulb-to-bulb distillation. The distilled oil was treated with water in dichloromethane to give 0.62 g (25%) of [2-((dimethylamino)methyl)-6-methylphenyl]boronic acid:  $^1\text{H}$  NMR ( $\text{CDCl}_3$ )  $\delta$  1.61 (s, 2H, -OH), 2.46 (s, 3H, 6-Me), 2.54 (s, 6H, *N*-Me), 3.81 (s, 2H, *N*-CH<sub>2</sub>), 6.88 (d,  $J$  = 7.4 Hz, 1H), 7.04 (t,  $J$  = 7.5 Hz, 1H), 7.12 (d,  $J$  = 7.4 Hz, 1H). This boronic acid was similarly treated with 0.69 g (3.22 mmol) of 1,1-diphenyl-1,2-ethanediol to give 0.81 g of 3 in 17% overall yield: mp 135.0–136.5 °C;  $^1\text{H}$  NMR ( $\text{CDCl}_3$ )  $\delta$  1.95 (s, 3H, 6-Me), 2.37 (s, 6H, *N*-Me), 3.87 (s, 2H, *N*-CH<sub>2</sub>), 4.78 (s, 2H, 4-CH<sub>2</sub>), 6.86 (d,  $J$  = 7.4 Hz, 1H), 7.96 (t,  $J$  = 7.5 Hz, 1H), 7.12 (d,  $J$  = 7.5 Hz, 1H), 7.15 (d,  $J$  = 7.2 Hz, 2H), 7.26 (t,  $J$  = 7.6 Hz, 4H), 7.54 (d,  $J$  = 7.7 Hz, 4H). Anal.

Calcd for  $\text{C}_{24}\text{H}_{26}\text{N}_2\text{BO}_2$ : C, 77.64; H, 7.06; N, 3.77. Found: C, 77.50; H, 7.15; N, 3.69.

**[2-((Dimethylamino)methyl)phenyl]diethylborane (4).** A suspension of [2-((dimethylamino)methyl)phenyl]lithium in ca. 50 mL of ether was prepared from 3.00 g (20.1 mmol) of *N,N*-dimethylbenzylamine and 15.8 mL (25.5 mmol) of 15% solution of butyllithium solution in hexane. To a three-necked flask charged with 10 mL of dry ether were slowly added the suspension of the lithium compound and 30 mL (30 mmol) of a 1.0 mol/L solution of diethylmethoxyborane in THF (Aldrich Co.) from respective dropping funnels at room temperature under a nitrogen atmosphere. The mixture was stirred for 20 h. The volatile materials were removed by evaporation under vacuum, and the residue was extracted with dichloromethane. The solvent was evaporated, and the crude material was purified by bulb-to-bulb distillation under reduced pressure to give 1.04 g (20%) of the desired compound as colorless oil: bp 125–126 °C (bath temp)/0.4 mmHg;  $^1\text{H}$  NMR ( $\text{CDCl}_3$ )  $\delta$  0.46 and 0.53 (AB of  $\text{ABX}_3$ ,  $J_{\text{AB}} = 13.7$ ,  $J_{\text{AX}} = 7.9$ ,  $J_{\text{BX}} = 7.5$  Hz, 4H, *B*-CH<sub>2</sub>), 0.82 (X of  $\text{ABX}_3$ , 6H, *B*-CH<sub>2</sub>CH<sub>3</sub>), 2.53 (s, 6H, *N*-Me), 3.91 (s, 2H, *N*-CH<sub>2</sub>), 7.02 (d,  $J$  = 7.5 Hz, 1H), 7.07 (dt,  $J$  = 1.0, 7.2 Hz, 1H), 7.16 (t,  $J$  = 7.2 Hz, 1H), 7.25 (d,  $J$  = 7.2 Hz, 1H);  $^{13}\text{C}$  NMR ( $\text{CDCl}_3$ )  $\delta$  9.8, 47.2 (*N*-Me), 68.4 (*N*-CH<sub>2</sub>), 121.4, 124.6, 126.5, 127.2, 130.0, 137.7 (aromatic carbons), where the methylene carbons of the ethyl groups were missing;  $^{11}\text{B}$  NMR ( $\text{CDCl}_3$ )  $\delta$  7.3 (line width  $h_{1/2}$  138 Hz). HRMS (FAB) calcd for  $\text{C}_{13}\text{H}_{22}^{11}\text{BN}$  ( $\text{MH}^+$ )  $m/e$  204.1924, found  $m/e$  204.1956.

**[2,6-Bis((dimethylamino)methyl)phenyl]diethylborane (5).** This compound was similarly prepared from [2,6-bis((dimethylamino)methyl)phenyl]lithium and diethylmethoxyborane. The reaction mixture was stirred for 23 h at room temperature followed by refluxing for 4 h. Distillation of the crude material gave the desired compound as colorless oil, which crystallized upon standing, in 32% yield: bp 142–143 °C (bath temp)/0.5 mmHg; mp 37–39 °C;  $^1\text{H}$  NMR ( $\text{CDCl}_3$ )  $\delta$  0.67 (q, 4H,  $J$  = 7.1 Hz, *B*-CH<sub>2</sub>), 0.81 (t, 6H,  $J$  = 7.5 Hz, *B*-CH<sub>2</sub>CH<sub>3</sub>), 2.42 (s, 12H, *N*-Me), 3.71 (s, 4H, *O*-CH<sub>2</sub>), 7.08 (t, 1H,  $J$  = 7.3 Hz, 4-H), 7.16 (d, 2H,  $J$  = 7.3 Hz, 3,5-H).  $^{13}\text{C}$  NMR ( $\text{CDCl}_3$ ):  $\delta$  10.6 (*B*-CH<sub>2</sub>CH<sub>3</sub>), 12.0 (br, *B*-CH<sub>2</sub>), 46.4 (*N*-Me), 65.5 (br, *N*-CH<sub>2</sub>), 123.3 (br), 124.9, 139.9, 153.7 (br, 1-C);  $^{11}\text{B}$  NMR ( $\text{CDCl}_3$ )  $\delta$  8.0 (line width  $h_{1/2}$  377 Hz). HRMS (FAB)  $\text{C}_{16}\text{H}_{27}\text{BN}_2$  ( $\text{MH}^+$ ) calcd  $m/e$  259.2345, found  $m/e$  259.2337.

**Dynamic NMR.** NMR spectra at various temperatures were measured on the JEOL spectrometer. Temperatures were read from a thermocouple equipped with the machine after the calibration with chemical shift differences of methanol protons. The samples were prepared by the dissolution of ca. 10 mg of a complex in 0.6 mL of an appropriate solvent. The total line shape analysis was performed by DNMR3K program<sup>36</sup> with an NEC-98 series computer. The line shapes were analyzed as an  $\text{ABX}_3 \rightleftharpoons \text{BAX}_3$  system for the ethyl methylene protons and as an  $\text{AB} \rightleftharpoons \text{BA}$  system for the other methylene protons. The line shapes of 5 were simulated as the exchange between two uncoupled singlets. Chemical shift differences and coupling constants were measured at several temperatures where the exchange rate was approximately zero. The chemical shift differences were linearly correlated with temperature, and the corrected values by extrapolation were used at the temperatures where line shapes changed. The coupling constants were independent of the temperature. Spin–spin relaxation times ( $T_2$ 's) were estimated from the line shapes at the slow-exchange limit and from the line widths of other signals which had no relation with the site exchange. The input parameters for the simulations and the rate constants can be obtained from the Supporting Information.

**Solid-State NMR.**  $^{13}\text{C}$  NMR spectra for the solid state of compound 2b were measured on a Bruker ARX-300 spectrom-

(36) A modified version of DNMR3 program<sup>37</sup> by Prof. H. Kihara of Hyogo University of Teacher Education for NEC personal computers.

(37) Binsch, G. *Top. Stereochem.* **1968**, 3, 97. Kleier, D.; Binsch, G. QCPE #165, Indiana University, Bloomington, IN.



**Table 4. Crystal and Structure Analysis Data for 2b**

formula	C <sub>26</sub> H <sub>31</sub> N <sub>2</sub> BO <sub>2</sub>
fw	414.35
cryst size (mm <sup>3</sup> )	0.45 × 0.20 × 0.15
cryst system	orthorhombic
space group	<i>Pbca</i>
<i>a</i> (Å)	20.591(3)
<i>b</i> (Å)	24.322(3)
<i>c</i> (Å)	9.195(2)
<i>Z</i>	8
<i>D<sub>c</sub></i> (g/cm <sup>3</sup> )	1.20
<i>μ</i> (Cu <i>Kα</i> ) (cm <sup>-1</sup> )	5.83
scan width (deg)	1.63 + 0.30 tan <i>θ</i>
no. of unique data	3900
no. of data used	2775 ( <i>F</i> <sub>0</sub> > 1.0σ( <i>F</i> ))
<i>R</i> ( <i>F</i> )	0.039
<i>R<sub>w</sub></i> ( <i>F</i> )	0.028

eter at 75.5 MHz with an MAS-DAB probe. The chemical shift was referred to the signal due the carbonyl carbon of glycine at 173.5 ppm. About 500 mg of fine powders was mounted in a cell made of zirconia (size 7 × 18 mm), and the spectra were collected under CPseltics mode with 4000 Hz spinning rate at room temperature. SSB signals were discriminated from the original signals by the measurements at various spinning rates. <sup>13</sup>C NMR (CPseltics): δ 44.5 and 48.0 (*N*-Me), 60.9 and 66.0 (*N*-CH<sub>2</sub>), 73.0 (*O*-CH<sub>2</sub>), 84.2 (*CPh*<sub>2</sub>), 121.0, 125.0, 128.9, 139.4, 143.4, 149.8 (aromatic carbons).

**X-ray Crystallography of 2b.** A crystal used for the measurements was grown from hexane–dichloromethane solutions. X-ray diffraction data were collected on a Rigaku AFC7R four-circle diffractometer with CuKα radiation (*λ* = 1.541 78 Å). The scan mode was the ω–2*θ* method, and the scan rate was 16.0 deg/min. Reflections were collected in the range of 2*θ* < 120°. The structures were solved by direct methods (SHELXS86)<sup>38</sup> and refined by full-matrix least-squares methods by using a teXsan program.<sup>39</sup> Anisotropic thermal parameters were employed for non-hydrogen atoms, and isotropic, for hydrogens. The reflection data were corrected for the Lorentz and polarization effects and secondary extinction. The function minimized was Σ[w(|*F*<sub>o</sub>| – |*F*<sub>c</sub>|)<sup>2</sup>], where *w* = (σ<sub>c</sub><sup>2</sup>|*F*<sub>o</sub>|)<sup>-1</sup>. Additional crystal and analysis data are listed in Table 4.

(38) Sheldrick, G. M. *Acta Crystallogr.* **1990**, *A46*, 467.

(39) *Crystal Structure Analysis Package*; Molecular Structure Corp.: The Woollands, TX, 1985 and 1992.

**Ab Initio Calculation.** Calculations were carried out with a CONVEX computer using the Gaussian 92 program.<sup>40</sup> For the model reactions comprised of borane and ammonia molecules, the structures at the original and the transition state were fully optimized with 6-31G\* basis set at the HF or MP<sup>41</sup> level, and the electronic energies were obtained at the MP level. The frequency analysis gave an imaginary value in wavenumbers for the 1:2 complex (**11**). For the calculations of the model compounds **12** and **15**, the structural optimization and the energy calculation were carried out at HF/3-21G\* level. The GIAO calculation<sup>42</sup> was carried out by the Gaussian 94 program.<sup>43</sup>

**Acknowledgment.** This work was partly supported by the Grant-in-Aid for Scientific Research No. 06740497 from the Ministry of Education, Science, Sports, and Culture of Japan and by a fund from the Japan Private School Promotion Foundation. The authors thank Dr. Katsuya Inoue of Kitasato University, Sagamiara, Japan, for the measurement of solid-state NMR.

**Supporting Information Available:** Tables of X-ray data (coordinates, bond distances, bond angles, and thermal parameters), data for the NMR line shape analysis, and total energies obtained by ab initio calculation and a figure of the solid-state <sup>13</sup>C NMR spectrum (7 pages). Ordering information is given on any current masthead page.

OM9803974

(40) Frisch, M. J.; Trucks, G. W.; Head-Gordon, M.; Gill, P. M. W.; Wong, M. W.; Foresman, J. B.; Johnson, B. G.; Schlegel, H. B.; Robb, M. A.; Replogle, E. S.; Gomperts, R.; Andres, J. L.; Raghavachari, K.; Binkley, J. S.; Gonzalez, C.; Martin, R. L.; Fox, D. J.; Defrees, D. J.; Baker, J.; Stewart, J. J. P.; Pople, J. A. *Gaussian 92*, revision C; Gaussian, Inc.: Pittsburgh, PA, 1992.

(41) Møller, C.; Plesset, M. S. *Phys. Rev.* **1934**, *46*, 618.

(42) Ditchfield, R. *Mol. Phys.* **1974**, *27*, 789. Wolinski, K.; Hilton, J. F.; Pulay, P. *J. Am. Chem. Soc.* **1990**, *112*, 8251.

(43) Frisch, M. J.; Trucks, G. W.; Schlegel, H. B.; Gill, P. M. W.; Johnson, B. G.; Robb, M. A.; Cheeseman, J. R.; Keith, T.; Petersson, G. A.; Montgomery, J. A.; Raghavachari, K.; Al-Laham, M. A.; Zakrzewski, V. G.; Ortiz, J. V.; Foresman, J. B.; Cioslowski, J.; Stefanov, B. B.; Nanayakkara, A.; Challacombe, M.; Peng, C. Y.; Ayala, P. Y.; Chen, W.; Wong, M. W.; Andres, J. L.; Replogle, E. S.; Gomperts, R.; Martin, R. L.; Fox, D. J.; Binkley, J. S.; Defrees, D. J.; Baker, J.; Stewart, J. P.; Head-Gordon, M.; Gonzalez, C.; Pople, J. A. *Gaussian 94*, revision D; Gaussian, Inc.: Pittsburgh, PA, 1995.